Autonomous Mid-Course Navigation for Lunar Return

Renato Zanetti*
The Charles Stark Draper Laboratory, Houston, Texas

A study of an autonomous lunar return navigation system is performed. Autonomy is achieved using optical sensors and celestial navigation. Sensors and error models for celestial navigation are developed with Monte Carlo methods and used to support the study. Sensitivity analysis of the estimation error to the sensors noises is obtained with linear covariance techniques.

I. Introduction

The Orion vehicle is required to autonomously return to Earth in a lunar mission if communication with the ground is lost. Ground tracking is the primary source of navigation to aid Orion for the Earth insertions burns as well as the mid course corrections. Clearly if communication is lost the ground tracking estimate cannot be used by the targeting system and Orion needs to rely in an alternative source of measurements. Optical navigation is the source of information in this emergency scenario. Orion cameras required to allow both terrain and celestial navigation. In low lunar orbit a camera will be pointed to the moon and information will be obtained by detecting the relative position of craters. This study focus on the navigation in cislunar space, when terrain navigation is not available. Orion's star cameras are required to be able to capture the Earth and moon as well as the stars. From this information two types of measurements are generated: the elevation of a star from the planet's limb and the angular radius of the planet.

This investigation focuses on the transfer from the moon to Earth. In the emergency situation where communication is lost the only objective is the safety of the crew, which translates into an acceptable flight-path angle at entry interface (EI). In this scenario the logical choice is a direct entry, as opposed to a nominal skip entry. A direct entry reduces the risk of the capsule bouncing back into space, and allows for a greater margin on the flight-path angle at EI.

The accuracy of the flight-path angle at EI is driven by several factors:

1. Navigation error at the time of the last mid-course burn.
2. Targeting error at the time of the last mid-course burn.
3. Burn execution error at the time of the last mid-course burn.
4. Trajectory perturbations between the last mid-course burn and EI.

Apollo missions had a maximum tolerable flight path angle at entry interface of ± 1 degree, with half of this error budget allocated to navigation. Using this same criteria, the navigation system at the time of targeting the last mid course correction must achieve a 3σ uncertainty of the flight path angle error mapped at entry interface of ± 0.5 degrees.

The primary objective of this paper is to model the sensors and analyze the navigation system to assure that the system meets the required performance.

A. Linear Covariance Analysis Methods

The main tool for this analysis is linear covariance analysis (LinCov). The linear covariance analysis follows the techniques presented in 1 and 2. For this analysis we have three states:

*Senior Member of the Technical Staff, GN&C Manned Space Systems, 17629 El Camino Real Suite 470, rzanetti@draper.com, AIAA Member.

1. Nominal state $\bar{\mathbf{x}}$
2. True state $\mathbf{x}$
3. Estimated state $\hat{\mathbf{x}}$

The nominal state is the design trajectory, in a perfect scenario, the GN&C system would be able to exactly match the true state to the nominal state. The difference between the true state and the nominal state is defined as the environment dispersion $\delta\mathbf{x}$

$$\delta\mathbf{x} \triangleq \mathbf{x} - \bar{\mathbf{x}}.$$

The difference between the estimated state and the nominal state is defined as the navigation dispersion $\delta\hat{\mathbf{x}}$

$$\delta\hat{\mathbf{x}} \triangleq \hat{\mathbf{x}} - \bar{\mathbf{x}}.$$

Finally, the difference between the true state and the estimated state, is defined as the estimation error $\mathbf{e}$ (also sometime referred to as the onboard error)

$$\mathbf{e} \triangleq \mathbf{x} - \hat{\mathbf{x}}.$$

Although it is possible to define the states with different lengths and elements, such a procedure is not necessary for this work.

Each state is allowed to evolve according to different models. Under standard Kalman filter assumptions, the difference between models is represented with zero-mean, white noise. The estimated state evolves as

$$\dot{\hat{\mathbf{x}}} = \mathbf{f}(\hat{\mathbf{x}}),$$

where $\mathbf{f}$ is a nonlinear function representing the system dynamics as modeled by the filter. The evolution of the nominal state is modeled as

$$\dot{\bar{\mathbf{x}}} = \mathbf{f}(\bar{\mathbf{x}}) + \boldsymbol{\upsilon},$$

where $\boldsymbol{\upsilon}$ reflects the fact that the dynamics model used to design the nominal trajectory is more complex than the navigation model used by the onboard computer. Under standard Kalman filter assumptions, the difference $\boldsymbol{\upsilon}$ is modeled as a zero-mean white process with spectral density $\hat{\mathbf{Q}}$. Therefore the evolution of the navigation dispersion can be approximated to first order as

$$\delta\dot{\hat{\mathbf{x}}} = \dot{\hat{\mathbf{x}}} - \dot{\bar{\mathbf{x}}} = \mathbf{f}(\bar{\mathbf{x}} + \delta\hat{\mathbf{x}}) - \mathbf{f}(\bar{\mathbf{x}}) - \boldsymbol{\upsilon} \simeq \mathbf{F}(\bar{\mathbf{x}})\delta\hat{\mathbf{x}} - \boldsymbol{\upsilon},$$

where $\mathbf{F}$ is the Jacobian of $\mathbf{f}$. Assuming all errors are zero mean, define the navigation covariance $\hat{\mathbf{P}}$ as

$$\hat{\mathbf{P}} \triangleq \mathrm{E}\left\{\delta\hat{\mathbf{x}}\,\delta\hat{\mathbf{x}}^{\mathrm{T}}\right\},$$

its evolution is governed by

$$\dot{\hat{\mathbf{P}}} = \mathbf{F}(\bar{\mathbf{x}})\hat{\mathbf{P}} + \hat{\mathbf{P}}\mathbf{F}(\bar{\mathbf{x}})^{\mathrm{T}} + \hat{\mathbf{Q}}.$$

Similarly, the true state is modeled to evolve as

$$\dot{\mathbf{x}} = \mathbf{f}(\mathbf{x}) + \boldsymbol{\nu}.$$

The evolution of the estimation error is given by

$$\dot{\mathbf{e}} = \dot{\mathbf{x}} - \dot{\hat{\mathbf{x}}} \simeq \mathbf{f}(\bar{\mathbf{x}}) + \mathbf{F}(\bar{\mathbf{x}})(\mathbf{x} - \bar{\mathbf{x}}) + \boldsymbol{\nu} - \mathbf{f}(\bar{\mathbf{x}}) - \mathbf{F}(\bar{\mathbf{x}})(\hat{\mathbf{x}} - \bar{\mathbf{x}}) = \mathbf{F}(\bar{\mathbf{x}})\mathbf{e} + \boldsymbol{\nu},$$

where $\boldsymbol{\nu}$ represents the unmodeled dynamics (the difference between the true dynamics and the filter model). The onboard covariance $\mathbf{P}$ evolves as

$$\dot{\mathbf{P}} = \mathbf{F}(\bar{\mathbf{x}})\mathbf{P} + \mathbf{P}\mathbf{F}(\bar{\mathbf{x}}) + \mathbf{Q},$$

where $\mathbf{Q}$ is the spectral density of the zero-mean, white process $\boldsymbol{\nu}$. Notice that the Jacobian $\mathbf{F}$ could be evaluated at the estimated state $\hat{\mathbf{x}}$ instead of the nominal state $\bar{\mathbf{x}}$, as in the extended Kalman filter.

Finally

$$\delta\dot{\mathbf{x}} \simeq \mathbf{F}(\bar{\mathbf{x}})\delta\mathbf{x} + \boldsymbol{\nu} - \boldsymbol{\upsilon}$$

the environment covariance $\bar{\mathbf{P}}$ is defined as the covariance of $\delta\mathbf{x}$ and evolves as

$$\dot{\bar{\mathbf{P}}} = \mathbf{F}(\bar{\mathbf{x}})\bar{\mathbf{P}} + \bar{\mathbf{P}}\mathbf{F}(\bar{\mathbf{x}}) + \bar{\mathbf{Q}},$$

notice that $\bar{\mathbf{Q}} = \mathbf{Q} + \hat{\mathbf{Q}}$ if $\boldsymbol{\nu}$ and $\boldsymbol{\upsilon}$ are assumed to be uncorrelated.

Since the environment and navigation dispersions are naturally correlated, it is intuitive to create an augmented dispersion state, whose covariance we defined as $\boldsymbol{\Pi}$

$$\boldsymbol{\Pi} \triangleq \mathrm{E}\left\{ \begin{bmatrix} \delta\mathbf{x} \\ \delta\hat{\mathbf{x}} \end{bmatrix} \begin{bmatrix} \delta\mathbf{x} \\ \delta\hat{\mathbf{x}} \end{bmatrix}^{\mathrm{T}} \right\} = \begin{bmatrix} \bar{\mathbf{P}} & \mathbf{C} \\ \mathbf{C}^{\mathrm{T}} & \hat{\mathbf{P}} \end{bmatrix}$$
$$\mathbf{C} \triangleq \mathrm{E}\left\{ \delta\mathbf{x}\, \delta\hat{\mathbf{x}}^{\mathrm{T}} \right\}.$$

The evolution of the augmented covariance is given by

$$\dot{\boldsymbol{\Pi}} = \begin{bmatrix} \mathbf{F}(\bar{\mathbf{x}}) & \mathbf{O}_{3\times3} \\ \mathbf{O}_{3\times3} & \mathbf{F}(\bar{\mathbf{x}}) \end{bmatrix} \boldsymbol{\Pi} \begin{bmatrix} \mathbf{F}(\bar{\mathbf{x}}) & \mathbf{O}_{3\times3} \\ \mathbf{O}_{3\times3} & \mathbf{F}(\bar{\mathbf{x}}) \end{bmatrix}^{\mathrm{T}} + \begin{bmatrix} \bar{\mathbf{Q}} & \hat{\mathbf{Q}} \\ \hat{\mathbf{Q}} & \hat{\mathbf{Q}} \end{bmatrix} \tag{1}$$

Eq. (1) assumes $\boldsymbol{\nu}$ and $\boldsymbol{\upsilon}$ are uncorrelated.

B. Rotation Conventions

The attitude is represented using a left rotation vector $\boldsymbol{\theta}$. Left rotations are used following the heritage from the Space Shuttle quaternion convention. The rotation vector represents the rotation from the inertial frame i to a body fixed frame b. The corresponding rotation matrix $\mathbf{T}_i^b$ is found as

$$\mathbf{T}_i^b = \mathbf{T}(\boldsymbol{\theta}) = \mathbf{I}_{3\times3} + \frac{\sin\theta}{\theta}[\boldsymbol{\theta}\times] + \frac{1-\cos\theta}{\theta^2}[\boldsymbol{\theta}\times]^2,$$

where $\theta = \|\boldsymbol{\theta}\|$, and $[\mathbf{a}\times]$ is the skew-symmetric matrix such that

$$[\mathbf{a}\times]\mathbf{b} = \mathbf{a}\times\mathbf{b} \;\; \forall \mathbf{a},\mathbf{b} \in \Re^3.$$

The attitude is the only state that is not integrated to obtain its nominal value. Instead, the nominal orientation always points the engines towards the sun. The attitude errors are defined in a multiplicative way, i.e.

$$\delta\boldsymbol{\theta} \triangleq \boldsymbol{\theta} \circ \bar{\boldsymbol{\theta}}^*, \qquad \delta\hat{\boldsymbol{\theta}} \triangleq \hat{\boldsymbol{\theta}} \circ \bar{\boldsymbol{\theta}}^*, \qquad \mathbf{e}_\theta \triangleq \boldsymbol{\theta} \circ \hat{\boldsymbol{\theta}}^*,$$

where the superscript asterisks represents the conjugate rotation $\boldsymbol{\theta}^*$=$-\boldsymbol{\theta}$, and $\circ$ represents the rotation vector composition, such that

$$\mathbf{T}(\boldsymbol{\theta}_1)\,\mathbf{T}(\boldsymbol{\theta}_2) = \mathbf{T}(\boldsymbol{\theta}_1 \circ \boldsymbol{\theta}_2).$$

Although the rotation vector composition is not implemented in the code, the advantage of these definitions is that the errors represent physical rotations. The attitude uncertainty is not computed but is fixed. The attitude dead-band during trans-Earth is 20 deg, which we model as the root sum square navigation dispersion being zero mean and $\pm$20 deg 3σ

$$\hat{\mathbf{P}}_{\theta\theta} \triangleq \mathrm{E}\left\{ \delta\hat{\boldsymbol{\theta}} \delta\hat{\boldsymbol{\theta}}^{\mathrm{T}} \right\} = \left(\frac{20\pi}{3\sqrt{3}\cdot 180} \right)^2 \mathbf{I}_{3\times3}.$$

The estimation error is modeled as zero mean with variance 0.1 deg in each axis

$$\mathbf{P}_{\theta\theta} \triangleq \mathrm{E}\left\{ \mathbf{e}_\theta \mathbf{e}_\theta^{\mathrm{T}} \right\} = \left(0.1\frac{\pi}{180} \right)^2 \mathbf{I}_{3\times3}.$$

The estimation error is given by given by

$$\mathbf{e}_\theta = \delta\boldsymbol{\theta} \circ \delta\hat{\boldsymbol{\theta}}^* \simeq \delta\boldsymbol{\theta} - \delta\hat{\boldsymbol{\theta}},$$

therefore

$$\mathbf{P}_{\theta\theta} \triangleq \mathrm{E}\left\{\delta\boldsymbol{\theta}\delta\boldsymbol{\theta}^{\mathrm{T}}\right\} = \bar{\mathbf{P}}_{\theta\theta} + \hat{\mathbf{P}}_{\theta\theta} - \mathrm{E}\left\{\delta\boldsymbol{\theta}\delta\hat{\boldsymbol{\theta}}^{\mathrm{T}}\right\} - \mathrm{E}\left\{\delta\hat{\boldsymbol{\theta}}\delta\boldsymbol{\theta}^{\mathrm{T}}\right\},$$

where

$$\mathrm{E}\left\{\delta\boldsymbol{\theta}\delta\hat{\boldsymbol{\theta}}^{\mathrm{T}}\right\} = \hat{\mathbf{P}}_{\theta\theta},$$

which results in the attitude environment dispersions having covariance

$$\bar{\mathbf{P}}_{\theta\theta} = \mathbf{P}_{\theta\theta} + \hat{\mathbf{P}}_{\theta\theta}.$$

II. Filter Definition and Dynamics

The state vector is composed by

$$\mathbf{x} = \begin{bmatrix}\mathbf{r}^{\mathrm{T}} & \mathbf{v}^{\mathrm{T}} & \boldsymbol{\theta}^{\mathrm{T}} & \mathbf{b}_m^{\mathrm{T}} & \boldsymbol{\sigma}_m^{\mathrm{T}} & \boldsymbol{\gamma}_m^{\mathrm{T}} & \mathbf{b}_r^{\mathrm{T}} & b_{st} & b_{ss,earth} & b_{ss,moon} & b_{h,earth} & b_{h,moon}\end{bmatrix}^{\mathrm{T}}$$

where position ($\mathbf{r}$) and velocity ($\mathbf{v}$) have conponent expressed in the Earth Centered Inertial frame, $\boldsymbol{\theta}$ is the rotation vector from the inertial frame to a body fixed frame, and the other states are errors to be defined later. The attitude dynamic is not modeled. The nominal attitude of engines pointing the sun is used with a constant uncertainty driven by the star-tracker. The star-tracker is not included in this analysis. Before star elevation measurements are taken, the vehicle slews to be able to acquire measurements. This attitude maneuver is assumed to be instantaneous, and it will add uncertainty in the translational states. After the batch of measurements are taken, the vehicle maneuvers back to its nominal attitude.

The acceleration of Orion with respect to a primary body P (either Earth or moon) accounting for Earth, moon, and sun gravitational fields is given by[3]

$$\begin{aligned}\ddot{\mathbf{r}}_{PV} = \ddot{\mathbf{r}}_V - \ddot{\mathbf{r}}_P &= -\frac{\mu_P}{r_{PV}^3}\mathbf{r}_{EV} - \frac{\mu_Q}{r_{QV}^3}\mathbf{r}_{QV} - \frac{\mu_S}{r_{SV}^3}\mathbf{r}_{SV} + \frac{\mu_Q}{r_{QP}^3}\mathbf{r}_{QP} + \frac{\mu_S}{r_{SP}^3}\mathbf{r}_{SP} \\ &= -\frac{\mu_P}{r_{PV}^3}\mathbf{r}_{PV} - \mu_Q\left[\frac{\mathbf{r}_{QV}}{r_{QV}^3} + \frac{\mathbf{r}_{PQ}}{r_{PQ}^3}\right] - \mu_S\left[\frac{\mathbf{r}_{SV}}{r_{SV}^3} + \frac{\mathbf{r}_{PS}}{r_{PS}^3}\right]\end{aligned} \tag{2}$$

where Q represents the secondary body (either moon or Earth). The relative positions of the celestial bodies are obtained from ephemeris files. Notice that Eq. (2) is not integrated directly but an Encke-Nystrom methodology is used instead.[3] The Encke-Nystrom method integrates the deviation from the two body orbit. Eq. (2) can be rewritten as

$$\ddot{\mathbf{r}}_{PV} = -\frac{\mu_P}{r_{PV}^3}\mathbf{r}_{PV} - \frac{\mu_Q}{r_{QV}^3}\left[f(q_Q)\mathbf{r}_{PQ} + \mathbf{r}_{PV}\right] - \frac{\mu_S}{r_{SV}^3}\left[f(q_S)\mathbf{r}_{PS} + \mathbf{r}_{PV}\right], \tag{3}$$

where

$$q_{(Q/S)} = \frac{\left(\mathbf{r}_{PV} - 2\mathbf{r}_{P(Q/S)}\right)\cdot\mathbf{r}_{PV}}{r_{P(Q/S)}^2} \qquad f(q) = \frac{3q + 3q^2 + q^3}{1 + (1+q)^{3/2}}. \tag{4}$$

The osculating orbit, is defined to be a solution of the two body problem

$$\ddot{\mathbf{r}}_{PV_{osc}} = -\frac{\mu_P}{r_{PV_{osc}}^3}\mathbf{r}_{PV_{osc}}, \tag{5}$$

and is computed along with the deviation from the osculating orbit $\boldsymbol{\delta}$

$$\ddot{\boldsymbol{\delta}} \triangleq \ddot{\mathbf{r}}_{PV} - \ddot{\mathbf{r}}_{PV_{osc}} = -\frac{\mu_P}{r_{PV_{osc}}^3}\boldsymbol{\delta} - \frac{\mu_P}{r_{PV_{osc}}^3}f(q)\mathbf{r}_{PV_{osc}} + \mathbf{a}, \tag{6}$$

where

$$q = \frac{(\boldsymbol{\delta} - 2\mathbf{r}_{PV})\cdot\boldsymbol{\delta}}{r_{PV}^2}.$$

and $f(q)$ is defined in Eq. (4). To propagate the trajectory in LinCov the perturbation from the two body problem $\mathbf{a}$ is given by

$$\mathbf{a} = -\frac{\mu_Q}{r_{QV}^3}\left[f(q_Q)\mathbf{r}_{PQ} + \mathbf{r}_{PV}\right] - \frac{\mu_S}{r_{SV}^3}\left[f(q_S)\mathbf{r}_{PS} + \mathbf{r}_{PV}\right].$$

All other states are modeled as first-order exponentially correlated random variables (ECRV), and they are assumed to be uncorrelated to each other. Notice that the Jacobian of the dynamics is used to compute the covariance of the error. Adding the distance between the moon and Earth (assumed perfectly known) to both the true state and the estimated state, will not change the error and its covariance. Therefore, it is irrelevant wether the primary body is the moon or the Earth. The dynamics partials are given by

$$\mathbf{F} = \begin{bmatrix} \mathbf{O}_{3\times3} & \mathbf{I}_{3\times3} & \mathbf{O}_{3\times15} \\ \mathbf{G}(\mathbf{r},\, t) & \mathbf{O}_{3\times3} & \mathbf{O}_{3\times15} \\ \mathbf{O}_{3\times3} & \mathbf{O}_{3\times3} & \mathbf{O}_{3\times15} \\ \mathbf{O}_{15\times3} & \mathbf{O}_{15\times3} & [\boldsymbol{\tau}\searrow] \end{bmatrix}$$

where matrix $[\boldsymbol{\tau}\searrow]$ is a diagonal matrix with the elements of $\boldsymbol{\tau}$ on the diagonal. The vector $\boldsymbol{\tau}$ contains the inverse of the time constant of each exponentially correlated random variables (ECRV) state. The Jacobian of the gravitational acceleration is obtained from Eq. (3)

$$\begin{aligned}\mathbf{G} = &\left(-\frac{\mu_P}{r_{PV}^3} - \frac{\mu_Q}{r_{QV}^3} - \frac{\mu_S}{r_{SV}^3}\right)\mathbf{I}_{3\times3} + 3\frac{\mu_P}{r_{PV}^5}\mathbf{r}_{PV}\mathbf{r}_{PV}^{\mathrm{T}} + 3\frac{\mu_Q}{r_{QV}^5}\left[f(q_Q)\mathbf{r}_{PQ} + \mathbf{r}_{PV}\right]\mathbf{r}_{QV}^{\mathrm{T}} + \\ &+ 3\frac{\mu_S}{r_{SV}^5}\left[f(q_S)\mathbf{r}_{PS} + \mathbf{r}_{PS}\right]\mathbf{r}_{SV}^{\mathrm{T}} - \frac{\mu_Q}{r_{QV}^3}\mathbf{r}_{PQ}\frac{\partial f(q_Q)}{\partial \mathbf{r}_{PV}} - \frac{\mu_S}{r_{SV}^3}\mathbf{r}_{PS}\frac{\partial f(q_S)}{\partial \mathbf{r}_{PV}},\end{aligned}$$

where

$$\frac{\partial f(q_{Q/S})}{\partial \mathbf{r}_{PV}} = \frac{\partial f(q_{Q/S})}{\partial q_{Q/S}}\frac{\partial q_{Q/S}}{\partial \mathbf{r}_{PV}}, \qquad \frac{\partial q_{Q/S}}{\partial \mathbf{r}_{PV}} = 2\frac{\mathbf{r}_{PV}^{\mathrm{T}} - \mathbf{r}_{P(Q/S)}^{\mathrm{T}}}{r_{P(Q/S)}^2}$$

$$\frac{\partial f}{\partial q} = 3\frac{1+2q+q^2}{1+(1+q)^{3/2}} - \frac{3}{2}\,\frac{3q+3q^2+q^3}{1+(1+q)^{3/2}}(1+q)^{1/2}.$$

III. Maneuvers

A. Translational Maneuvers

During the trans-Earth phase, six maneuvers occur. These maneuvers are modeled as impulsive, and provide an instantaneous change in the spacecraft's velocity. Given the estimated position and velocity, the targeting algorithm provides a nominal change in velocity in the inertial frame $\Delta\mathbf{v}_{nom}^i(\hat{\mathbf{r}}, \hat{\mathbf{v}})$. Since the burn is perform by effectors mounted on the vehicle the inertial $\Delta\mathbf{v}$ is rotated into the body frame using the estimated attitude. The maneuver execution errors are expressed in a body fixed frame, these errors include the maneuver bias $\mathbf{b}_m$, the maneuver scale factors $\boldsymbol{\sigma}_m$, and the maneuver misalignment errors $\boldsymbol{\gamma}_m$. Hence the true maneuver is given by

$$\Delta\mathbf{v}^i = \mathbf{T}_b^i\,\mathbf{T}(\boldsymbol{\gamma}_m)\left\{(\mathbf{I} + [\boldsymbol{\sigma}_m\searrow])\hat{\mathbf{T}}_i^b\Delta\mathbf{v}_{nom}^i(\hat{\mathbf{r}}, \hat{\mathbf{v}}) + \mathbf{b}_m\right\} + \boldsymbol{\mu}, \tag{7}$$

where $\boldsymbol{\mu}$ is a zero-mean random error with covariance $\mathbf{M}$, matrix $\mathbf{T}(\boldsymbol{\gamma}_m)$ is the direction cosines matrix parameterizing the rotation vector $\boldsymbol{\gamma}_m$, matrix $[\boldsymbol{\sigma}_m\searrow]$ is a diagonal matrix with the elements of vector $\boldsymbol{\sigma}_m$ on the diagonal, and

$$\hat{\mathbf{T}}_i^b \triangleq \mathbf{T}(\hat{\boldsymbol{\theta}}) \qquad \mathbf{T}_i^b \triangleq \mathbf{T}(\boldsymbol{\theta}),$$

where $\boldsymbol{\theta}$ is the true rotation vector taking the inertial frame into the body fixed frame. Notice that Eq. (7) is the only instance in which the true quantities are affected by estimated quantities. Through the thrusters we are able to modify the true state, and by doing so we want to reduce the environment dispersions.

Similar to Eq. (7), the estimated change in velocity is given by

$$\Delta\hat{\mathbf{v}}^i = \hat{\mathbf{T}}_b^i\,\mathbf{T}(\hat{\boldsymbol{\gamma}}_m)\left\{(\mathbf{I} + [\hat{\boldsymbol{\sigma}}_m\searrow])\hat{\mathbf{T}}_i^b\Delta\mathbf{v}_{nom}^i(\hat{\mathbf{r}}, \hat{\mathbf{v}}) + \hat{\mathbf{b}}_m\right\}.$$

Define $\mathbf{v}^{+c}$ to be the true velocity immediately after the correction burn, and $\mathbf{v}^{-c}$ the true velocity immediately before the correction burn,

$$\mathbf{v}^{+c} = \mathbf{v}^{-c} + \Delta\mathbf{v}^i.$$

Similarly, for the estimated state

$$\hat{\mathbf{v}}^{+c} = \hat{\mathbf{v}}^{-c} + \Delta\hat{\mathbf{v}}^{i}.$$

Expanding the contribution to the estimation error due to the maneuver in a Taylor series centered at $\mathbf{x} = \bar{\mathbf{x}}$, and truncating the series to first order, we obtain

$$\begin{aligned}
\Delta\mathbf{v}^{i} - \Delta\hat{\mathbf{v}}^{i} &= \bar{\mathbf{T}}_b^i\mathbf{T}(\delta\boldsymbol{\theta})^{\mathrm{T}}\mathbf{T}(\delta\boldsymbol{\gamma}_m)\mathbf{T}(\bar{\boldsymbol{\gamma}}_m)\left\{(\mathbf{I} + [\bar{\boldsymbol{\sigma}}_m\diagdown] + [\delta\boldsymbol{\sigma}_m\diagdown])\mathbf{T}(\delta\hat{\boldsymbol{\theta}})\bar{\mathbf{T}}_i^b\Delta\mathbf{v}_{nom}^{i}(\hat{\mathbf{r}},\hat{\mathbf{v}}) + \bar{\mathbf{b}}_m + \delta\mathbf{b}_m\right\} + \boldsymbol{\mu} \\
&\quad - \bar{\mathbf{T}}_b^i\mathbf{T}(\delta\hat{\boldsymbol{\theta}})^{\mathrm{T}}\mathbf{T}(\delta\hat{\boldsymbol{\gamma}}_m)\mathbf{T}(\bar{\boldsymbol{\gamma}}_m)\left\{(\mathbf{I} + [\bar{\boldsymbol{\sigma}}_m\diagdown] + [\delta\hat{\boldsymbol{\sigma}}_m\diagdown])\mathbf{T}(\delta\hat{\boldsymbol{\theta}})\bar{\mathbf{T}}_i^b\Delta\mathbf{v}_{nom}^{i}(\hat{\mathbf{r}},\hat{\mathbf{v}}) + \bar{\mathbf{b}}_m + \delta\hat{\mathbf{b}}_m\right\} \\
&\simeq \mathbf{D}\mathbf{e}^{-c} + \boldsymbol{\mu},
\end{aligned}$$

where $\mathbf{e}^{-c}$ is the estimation error immediately before the correction burn. Including only the active states

$$\begin{aligned}
\mathbf{x} &= \begin{bmatrix}\mathbf{r}^{\mathrm{T}} & \mathbf{v}^{\mathrm{T}} & \boldsymbol{\theta}^{\mathrm{T}} & \mathbf{b}_m^{\mathrm{T}} & \boldsymbol{\sigma}_m^{\mathrm{T}} & \boldsymbol{\gamma}_m^{\mathrm{T}}\end{bmatrix}^{\mathrm{T}} \\
\mathbf{D} &= \begin{bmatrix}\mathbf{O}_{3\times3} & \mathbf{O}_{3\times3} & \mathbf{D}_\theta & \bar{\mathbf{T}}_b^i\mathbf{T}(\bar{\boldsymbol{\gamma}}_m) & \bar{\mathbf{T}}_b^i\mathbf{T}(\bar{\boldsymbol{\gamma}}_m)[\bar{\mathbf{T}}_i^b\Delta\mathbf{v}_{nom}(\bar{\mathbf{r}},\bar{\mathbf{v}})\diagdown] & \mathbf{D}_\gamma\end{bmatrix} \\
\mathbf{D}_\gamma &= -\bar{\mathbf{T}}_b^i\left[\mathbf{T}(\bar{\boldsymbol{\gamma}}_m)\left\{(\mathbf{I} + [\bar{\boldsymbol{\sigma}}_m\diagdown])\bar{\mathbf{T}}_i^b\Delta\mathbf{v}_{nom}(\bar{\mathbf{r}},\bar{\mathbf{v}}) + \bar{\mathbf{b}}_m\right\}\times\right] \\
\mathbf{D}_\theta &= \bar{\mathbf{T}}_b^i\left[\mathbf{T}(\bar{\boldsymbol{\gamma}}_m)\left\{(\mathbf{I} + [\bar{\boldsymbol{\sigma}}_m\diagdown])\bar{\mathbf{T}}_i^b\Delta\mathbf{v}_{nom}(\bar{\mathbf{r}},\bar{\mathbf{v}}) + \bar{\mathbf{b}}_m\right\}\times\right],
\end{aligned}$$

where the maneuver misalignment estimation error $\mathbf{e}_{\gamma_m}$ is defined as a rotation vector, i.e.

$$\mathbf{T}(\mathbf{e}_{\gamma_m}) \triangleq \mathbf{T}(\boldsymbol{\gamma}_m)\mathbf{T}(\hat{\boldsymbol{\gamma}}_m)^{\mathrm{T}}.$$

The estimation error immediately after the correction burn is given by

$$\mathbf{e}^{+c} = \mathbf{e}^{-c} + \mathbf{V}\mathbf{D}\mathbf{e}^{-c} + \mathbf{V}\boldsymbol{\mu}$$

where

$$\mathbf{V} = \begin{bmatrix}\mathbf{O}_{3\times3}\\ \mathbf{I}_{3\times3}\\ \mathbf{O}_{12\times3}\end{bmatrix}.$$

The change in the onboard covariance due to the maneuver is given by

$$\mathbf{P}^{+c} = (\mathbf{I} + \mathbf{V}\mathbf{D})\mathbf{P}^{-c}(\mathbf{I} + \mathbf{V}\mathbf{D})^{\mathrm{T}} + \mathbf{V}\mathbf{M}\mathbf{V}^{\mathrm{T}}.$$

The nominal correction maneuver is given by

$$\Delta\bar{\mathbf{v}} = \bar{\mathbf{T}}_b^i\,\mathbf{T}(\bar{\boldsymbol{\gamma}}_m)\left\{(\mathbf{I} + [\bar{\boldsymbol{\sigma}}_m\diagdown])\bar{\mathbf{T}}_i^b\Delta\mathbf{v}_{nom}(\bar{\mathbf{r}},\bar{\mathbf{v}}) + \bar{\mathbf{b}}_m\right\}, \tag{8}$$

where the nominal bias, misalignment, and scale factor are set to zero reducing Eq. (8) to

$$\Delta\bar{\mathbf{v}} = \Delta\mathbf{v}_{nom}(\bar{\mathbf{r}},\bar{\mathbf{v}}).$$

The contribution to the navigation dispersions due to the maneuver is

$$\Delta\hat{\mathbf{v}} - \Delta\bar{\mathbf{v}} \simeq \hat{\mathbf{D}}\delta\hat{\mathbf{x}}.$$

where

$$\begin{aligned}
\hat{\mathbf{D}} &= \mathbf{D} + \hat{\mathbf{D}}_{rv\theta} \\
\hat{\mathbf{D}}_{rv\theta} &= \bar{\mathbf{T}}_b^i\,\mathbf{T}(\bar{\boldsymbol{\gamma}}_m)(\mathbf{I} + [\bar{\boldsymbol{\sigma}}_m\diagdown])\left[\bar{\mathbf{T}}_i^b\,\tfrac{\partial\Delta\mathbf{v}_{nom}}{\partial\mathbf{r}}\big|_{\bar{\mathbf{r}}} \quad \bar{\mathbf{T}}_i^b\,\tfrac{\partial\Delta\mathbf{v}_{nom}}{\partial\mathbf{v}}\big|_{\bar{\mathbf{v}}} \quad \hat{\mathbf{D}}_\theta \quad \mathbf{O}_{3\times9}\right] \\
\hat{\mathbf{D}}_\theta &= -[\bar{\mathbf{T}}_i^b\Delta\mathbf{v}_{nom}(\bar{\mathbf{r}},\bar{\mathbf{v}})\times].
\end{aligned}$$

The contribution to the environment dispersions due to the maneuver is

$$\Delta\mathbf{v} - \Delta\bar{\mathbf{v}} \simeq \mathbf{D}\delta\mathbf{x} + \hat{\mathbf{D}}_{rv\theta}\delta\hat{\mathbf{x}} + \boldsymbol{\mu}.$$

Notice that the environmental dispersions are naturally coupled with the navigation dispersions. The maneuvers are the only instances in which we can reduce the environmental dispersions since they are computed through the estimated state. The change in the augmented dispersions covariance due to the maneuver is then given by

$$\boldsymbol{\Pi}^{+c} = \begin{bmatrix}\mathbf{I} + \mathbf{V}\mathbf{D} & \mathbf{V}\hat{\mathbf{D}}_{rv\theta}\\ \mathbf{O}_{3\times3} & \mathbf{I} + \mathbf{V}\hat{\mathbf{D}}\end{bmatrix}\boldsymbol{\Pi}^{-c}\begin{bmatrix}\mathbf{I} + \mathbf{V}\mathbf{D} & \mathbf{V}\hat{\mathbf{D}}_{rv\theta}\\ \mathbf{O}_{3\times3} & \mathbf{I} + \mathbf{V}\hat{\mathbf{D}}\end{bmatrix}^{\mathrm{T}} + \begin{bmatrix}\mathbf{V}\mathbf{M}\mathbf{V}^{\mathrm{T}} & \mathbf{O}_{3\times3}\\ \mathbf{O}_{3\times3} & \mathbf{O}_{3\times3}\end{bmatrix}.$$

B. Rotational Maneuvers

The nominal CEV orientation points the thrusters towards the Sun to maximize the solar arrays energy production and for other thermal advantages. From an optical navigation standpoint however, such an orientation is not ideal because it generally does not allow for the star cameras to point towards the Earth or moon to obtain measurements. Therefore, if the ground updates were not available, it would be necessary to perform attitude maneuvers before each burn. These maneuvers would point the cameras towards the Earth or moon to collect the measurements. After a sufficient number of measurements are acquired to reduce the navigation uncertainty, the vehicle would maneuver back to its nominal attitude or to its burn attitude. These attitude maneuvers will increase the uncertainty in both the orientation and the velocity of the vehicle. The uncertainty in Orion's orientation is not calculated, therefore we are only interested in the velocity uncertainty due to the rotational maneuvers. The forces applied will not create only torque, but will have some residual value that will induce a $\Delta\mathbf{v}$. The true change in velocity due to rotational maneuver $\Delta\mathbf{v}_r$ is modeled as

$$\Delta\mathbf{v}_r = \mathbf{T}_b^i\mathbf{b}_r + \boldsymbol{\zeta},$$

where $\mathbf{b}_r$ is a bias expressed in the body frame. The estimated perturbation is

$$\Delta\hat{\mathbf{v}}_r = \hat{\mathbf{T}}_b^i\hat{\mathbf{b}}_r,$$

from which we obtain that

$$\Delta\mathbf{v}_r - \Delta\hat{\mathbf{v}}_r = \bar{\mathbf{T}}_b^i[\bar{\mathbf{b}}_r\times]\mathbf{e}_\theta + \bar{\mathbf{T}}_b^i\mathbf{e}_{b_r} + \boldsymbol{\zeta}.$$

Including only the active states

$$\mathbf{x} = \begin{bmatrix}\mathbf{r}^{\mathrm{T}} & \mathbf{v}^{\mathrm{T}} & \boldsymbol{\theta}^{\mathrm{T}} & \mathbf{b}_r^{\mathrm{T}}\end{bmatrix}^{\mathrm{T}},$$

the contribution to the estimation error from the rotational maneuvers is given by

$$\mathbf{e}^{+r} = \mathbf{e}^{-r} + \begin{bmatrix}\mathbf{0}_{3\times1}\\ \bar{\mathbf{T}}_b^i[\bar{\mathbf{b}}_r\times]\mathbf{e}_\theta + \bar{\mathbf{T}}_b^i\mathbf{e}_{b_r}\\ \mathbf{0}_{6\times1}\end{bmatrix} + \begin{bmatrix}\mathbf{0}_{3\times1}\\ \boldsymbol{\zeta}\\ \mathbf{0}_{6\times1}\end{bmatrix} = (\mathbf{I}+\mathbf{E})\,\mathbf{e}^{-r} + \begin{bmatrix}\mathbf{0}_{3\times1}\\ \boldsymbol{\zeta}\\ \mathbf{0}_{6\times1}\end{bmatrix},$$

from which we obtain that

$$\mathbf{P}^{+r} = (\mathbf{I}+\mathbf{E})\,\mathbf{P}^{-r}\,(\mathbf{I}+\mathbf{E})^{\mathrm{T}} + \mathbf{N}.$$

The nominal perturbation is

$$\Delta\bar{\mathbf{v}}_r = \bar{\mathbf{T}}_b^i\bar{\mathbf{b}}_r,$$

the change in augmented dispersions covariance is given by

$$\boldsymbol{\Pi}^{+r} = \begin{bmatrix}\mathbf{I}+\mathbf{E} & \mathbf{O}_{12\times12}\\ \mathbf{O}_{12\times12} & \mathbf{I}+\mathbf{E}\end{bmatrix}\boldsymbol{\Pi}^{-r}\begin{bmatrix}\mathbf{I}+\mathbf{E} & \mathbf{O}_{12\times12}\\ \mathbf{O}_{12\times12} & \mathbf{I}+\mathbf{E}\end{bmatrix}^{\mathrm{T}} + \begin{bmatrix}\mathbf{N} & \mathbf{O}_{12\times12}\\ \mathbf{O}_{12\times12} & \mathbf{O}_{12\times12}\end{bmatrix}.$$

IV. Filter Update

The update of the estimated state due to a measurement $\mathbf{y}$, is that of the Kalman filter where

$$\mathbf{y} = \mathbf{h}(\mathbf{x}) + \boldsymbol{\eta},$$

where $\boldsymbol{\eta}$ is zero mean, white, and has covariance $\mathbf{R}$. The estimated state is updated as

$$\hat{\mathbf{x}}^+ = \hat{\mathbf{x}}^- + \mathbf{K}\left(\mathbf{y} - \mathbf{h}(\hat{\mathbf{x}})\right),$$

using a Taylor series expansion centered in $\bar{\mathbf{x}}$

$$\mathbf{e}^+ \simeq \mathbf{e}^- + \mathbf{K}\left(\boldsymbol{\eta} - \mathbf{H}\mathbf{e}^-\right),$$

matrix $\mathbf{H}$ is the Jacobian of $\mathbf{h}$ evaluated at the nominal state. The onboard error covariance update is given by

$$\mathbf{P}^{+} = (\mathbf{I} - \mathbf{KH})\,\mathbf{P}^{-}\,(\mathbf{I} - \mathbf{KH})^{\mathrm{T}} + \mathbf{KRK}^{\mathrm{T}},$$

where the optimal Kalman gain is

$$\mathbf{K} = \mathbf{P}^{-}\mathbf{H}^{\mathrm{T}}\left(\mathbf{HP}^{-}\mathbf{H}^{\mathrm{T}} + \mathbf{R}\right).$$

The true and nominal states remain unchanged trough measurements, therefore the environment dispersion remains the same.

$$\delta\mathbf{x}^{+} = \delta\mathbf{x}^{-}.$$

The navigation dispersion is updated according to

$$\delta\hat{\mathbf{x}}^{+} = \hat{\mathbf{x}}^{+} - \bar{\mathbf{x}} = \hat{\mathbf{x}}^{-} + \mathbf{K}\left(\mathbf{y} - \mathbf{h}(\hat{\mathbf{x}})\right) - \bar{\mathbf{x}} \simeq \delta\hat{\mathbf{x}}^{-} + \mathbf{K}\left(\mathbf{h}(\bar{\mathbf{x}}) + \mathbf{H}\delta\mathbf{x} + \boldsymbol{\eta} - \mathbf{h}(\bar{\mathbf{x}}) - \mathbf{H}\delta\hat{\mathbf{x}}^{-}\right)$$

Therefore the dispersions covariances update according to

$$\boldsymbol{\Pi}^{+} = \begin{bmatrix} \mathbf{I} & \mathbf{O} \\ \mathbf{KH} & (\mathbf{I} - \mathbf{KH}) \end{bmatrix} \boldsymbol{\Pi}^{-} \begin{bmatrix} \mathbf{I} & \mathbf{O} \\ \mathbf{KH} & (\mathbf{I} - \mathbf{KH}) \end{bmatrix}^{\mathrm{T}} + \begin{bmatrix} \mathbf{O} & \mathbf{O} \\ \mathbf{O} & \mathbf{KRK}^{\mathrm{T}} \end{bmatrix}.$$

The optical measurements available to update the state in cislunar space are the star elevation from the planetary limb and the apparent planet radius, as shown in Figure 1.

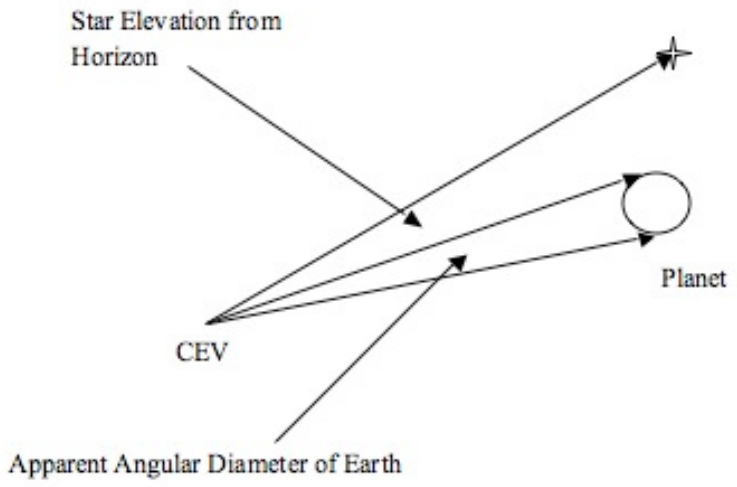

Figure 1. Optical measurements available for Cislunar navigation

A. Star-Horizon Elevation Measurement

The model for the star-horizon measurement is based on Battin,[4] but the measurement errors are different and introduced in alternative ways. The apparent direction of the star is

$$\mathbf{i}_s^{*} = \mathrm{Unit}(\mathbf{i}_s + \frac{\mathbf{v}_{sv}}{c}),$$

where the notation $\mathrm{Unit}(\mathbf{v})$ means the unit vector with the same direction of vector $\mathbf{v}$. Vector $\mathbf{v}_{sv}$ is the velocity of the vehicle with respect of the sun, c is the speed of light, and $\mathbf{i}_s$ is the direction of the star already accounted for the relative velocity between the sun and the star. The apparent direction of the horizon is given by

$$\mathbf{i}_h^{*} = \mathrm{Unit}(\mathbf{i}_h + \frac{\mathbf{v}_{pv}}{c}),$$

where $\mathbf{v}_{pv}$ is the velocity of the vehicle with respect to the body we are using to take the elevation measurements (Earth or moon).

$$\mathbf{i}_h = \text{Unit}(\mathbf{r}_h - \mathbf{r})$$

is the unit vector defining the direction of the horizon with respect to the vehicle. The perfect star elevation measurement is given by

$$y^\star_{se} = \arccos(\mathbf{i}^*_h \cdot \mathbf{i}^*_s)$$

Three error sources are modeled, each having both bias and noise. The first source of error is the precision of the star camera. The noise is η_{sc} and the bias is b_{sc}. The other two sources of error are shown in Figure 2 The second source of error is the identification of the substellar point along the planets horizon, with bias

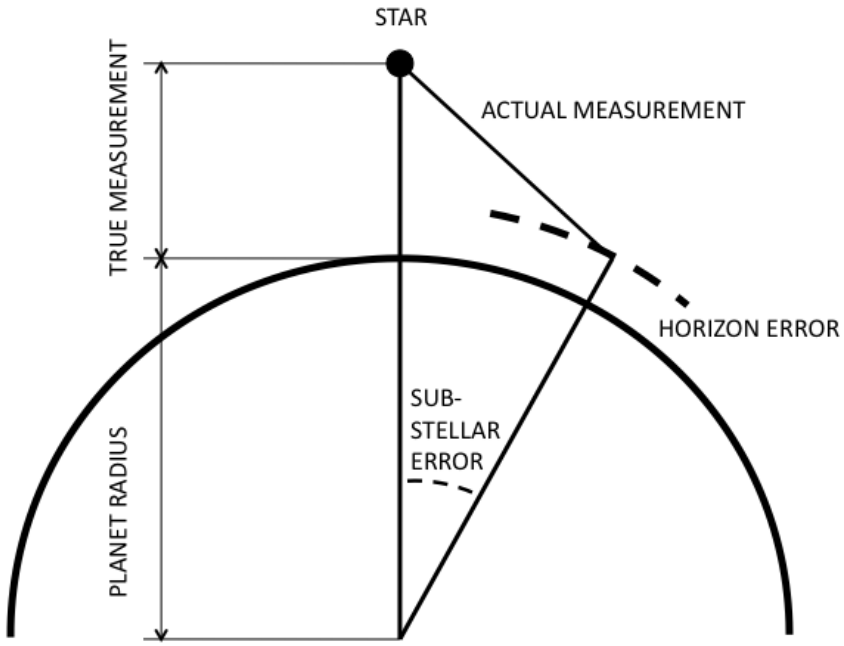

Figure 2. Horizon-Star elevation measurement errors

b_{ss} and noise η_{ss} are modeled. Finally there is the error in determining the altitude horizon, whose bias is b_h and noise is η_h. The measurement model is obtained using the cosine law and is given by

$$y_{se} = \left[\left(y^\star_{se} + \arcsin \frac{R_p}{r_{pv}} \right)^2 + \left(\arcsin \frac{R_p}{r_{pv}} + \arcsin \frac{b_h + \eta_h}{r_{pv}} \right)^2 + \right.$$
$$\left. - 2 \left(y^\star_{se} + \arcsin \frac{R_p}{r_{pv}} \right) \left(\arcsin \frac{R_p}{r_{pv}} + \arcsin \frac{b_h + \eta_h}{r_{pv}} \right) \cos(b_{ss} + \eta_{ss}) \right]^{\frac{1}{2}} + b_{sc} + \eta_{sc}, \tag{9}$$

where R_p is the planet's diameter, and r_{pv} is the distance between the planet and Orion. The nominal measurement is given by

$$\bar{y}_{se} = \left[\left(\bar{y}^\star_{se} + \arcsin \frac{R_p}{\bar{r}_{pv}} \right)^2 + \left(\arcsin \frac{R_p}{\bar{r}_{pv}} + \arcsin \frac{\bar{b}_h}{\bar{r}_{pv}} \right)^2 + \right.$$
$$\left. - 2 \left(\bar{y}^\star_{se} + \arcsin \frac{R_p}{\bar{r}_{pv}} \right) \left(\arcsin \frac{R_p}{\bar{r}_{pv}} + \arcsin \frac{\bar{b}_h}{\bar{r}_{pv}} \right) \cos \bar{b}_{ss} \right]^{\frac{1}{2}} + \bar{b}_{sc}$$

Including only the active states

$$\mathbf{x}^{\mathrm{T}} = \begin{bmatrix} \mathbf{r}^{\mathrm{T}} & \mathbf{v}^{\mathrm{T}} & b_{st} & b_{ss} & b_h \end{bmatrix} \qquad \mathbf{e} = \mathbf{x} - \hat{\mathbf{x}},$$

the measurement partials are defined as

$$\mathbf{H}_{se} = \left.\frac{\partial y_{se}}{\partial \mathbf{x}}\right|_{\mathbf{x}=\bar{\mathbf{x}},\boldsymbol{\eta}_{se}=\mathbf{0}} \qquad \mathbf{L}_{se} = \left.\frac{\partial y_{se}}{\partial \boldsymbol{\eta}_{se}}\right|_{\mathbf{x}=\bar{\mathbf{x}},\boldsymbol{\eta}_{se}=\mathbf{0}}$$

where

$$\boldsymbol{\eta}_{se} = \begin{bmatrix} \eta_{st} \\ \eta_{ss} \\ \eta_h \end{bmatrix}.$$

From Eq. (9) we obtain the measurement partials

$$\begin{aligned}
\mathbf{H}_{se}(1:3) &= \left.\left(\frac{\partial y_{se}}{\partial y^{\star}_{se}}\frac{\partial y^{\star}_{se}}{\partial \mathbf{r}} + \frac{\partial y_{se}}{\partial r_{pv}}\frac{\partial r_{pv}}{\partial \mathbf{r}}\right)\right|_{\mathbf{x}=\bar{\mathbf{x}},\boldsymbol{\eta}_{se}=\mathbf{0}} \\
\mathbf{H}_{se}(3:6) &= \left.\frac{\partial y_{se}}{\partial y^{\star}_{se}}\frac{\partial y^{\star}_{se}}{\partial \mathbf{v}}\right|_{\mathbf{x}=\bar{\mathbf{x}},\boldsymbol{\eta}_{se}=\mathbf{0}} \\
\mathbf{H}_{se}(7) &= 1 \\
\mathbf{H}_{se}(8) &= \frac{1}{\bar{y}_{se} - \bar{b}_{st}}\left[\left(\bar{y}^{\star}_{se} + \arcsin\frac{R_p}{\bar{r}_{pv}}\right)\left(\arcsin\frac{R_p}{\bar{r}_{pv}} + \arcsin\frac{\bar{b}_h}{\bar{r}_{pv}}\right)\sin\bar{b}_{ss}\right] \\
\mathbf{H}_{se}(9) &= \frac{1}{\bar{y}_{se} - \bar{b}_{st}}\left[\left(\arcsin\frac{R_p}{\bar{r}_{pv}} + \arcsin\frac{\bar{b}_h}{\bar{r}_{pv}}\right) - \left(\bar{y}^{\star}_{se} + \arcsin\frac{R_p}{\bar{r}_{pv}}\right)\cos\bar{b}_{ss}\right]\left(\bar{r}^2_{pv} - \bar{b}^2_h\right)^{-\frac{1}{2}} \\
\mathbf{L}_{se}(1) &= 1 \\
\mathbf{L}_{se}(2) &= \frac{1}{\bar{y}_{se} - \bar{b}_{st}}\left[\left(\bar{y}^{\star}_{se} + \arcsin\frac{R_p}{\bar{r}_{pv}}\right)\left(\arcsin\frac{R_p}{\bar{r}_{pv}} + \arcsin\frac{\bar{b}_h}{\bar{r}_{pv}}\right)\sin\bar{b}_{ss}\right] \\
\mathbf{L}_{se}(3) &= \frac{1}{\bar{y}_{se} - \bar{b}_{st}}\left[\left(\arcsin\frac{R_p}{\bar{r}_{pv}} + \arcsin\frac{\bar{b}_h}{\bar{r}_{pv}}\right) - \left(\bar{y}^{\star}_{se} + \arcsin\frac{R_p}{\bar{r}_{pv}}\right)\cos\bar{b}_{ss}\right]\left(\bar{r}^2_{pv} - \bar{b}^2_h\right)^{-\frac{1}{2}}.
\end{aligned}$$

To calculate the partials with respect to position and velocity we use

$$\begin{aligned}
\frac{\partial y_{se}}{\partial y^{\star}_{se}} &= \frac{1}{\bar{y}_{se} - \bar{b}_{st}}\left[\left(\bar{y}^{\star}_{se} + \arcsin\frac{R_p}{\bar{r}_{pv}}\right) - \left(\arcsin\frac{R_p}{\bar{r}_{pv}} + \arcsin\frac{\bar{b}_h}{\bar{r}_{pv}}\right)\cos\bar{b}_{ss}\right] \\
\frac{\partial y_{se}}{\partial r_{pv}} &= -\frac{1}{\bar{r}^2_{pv}}\frac{1}{\bar{y}_{se} - \bar{b}_{st}}\left\{\left(\bar{y}^{\star}_{se} + \arcsin\frac{R_p}{\bar{r}_{pv}}\right)\bar{r}_{pv}(\bar{r}^2_{pv} - R^2_p)^{-\frac{1}{2}}R_p + \right. \\
&\quad + \left(\arcsin\frac{R_p}{\bar{r}_{pv}} + \arcsin\frac{\bar{b}_h}{\bar{r}_{pv}}\right)\left[\bar{r}_{pv}(\bar{r}^2_{pv} - R^2_p)^{-\frac{1}{2}}R_p + \left(\bar{r}^2_{pv} - \bar{b}^2_h\right)^{-\frac{1}{2}}\bar{b}_h\bar{r}_{pv}\right] + \\
&\quad - \left[\bar{r}_{pv}(\bar{r}^2_{pv} - R^2_p)^{-\frac{1}{2}}R_p\left(\arcsin\frac{R_p}{\bar{r}_{pv}} + \arcsin\frac{\bar{b}_h}{\bar{r}_{pv}}\right) + \right. \\
&\quad \left.\left. + \left(\bar{y}^{\star}_{se} + \arcsin\frac{R_p}{\bar{r}_{pv}}\right)\left[\bar{r}_{pv}(\bar{r}^2_{pv} - R^2_p)^{-\frac{1}{2}}R_p + \left(\bar{r}^2_{pv} - \bar{b}^2_h\right)^{-\frac{1}{2}}\bar{b}_h\bar{r}_{pv}\right)\right]\cos\bar{b}_{ss}\right\} \\
\frac{\partial r_{pv}}{\partial \mathbf{r}} &= \frac{1}{r_{pv}}\mathbf{r}^{\mathrm{T}},
\end{aligned}$$

the partials of the unit vectors are

$$\begin{aligned}
\frac{\partial \mathbf{i}_s^*}{\partial \mathbf{r}} &= \mathbf{0} \\
\frac{\partial \mathbf{i}_h^*}{\partial \mathbf{r}} &= -\left[\bar{\mathbf{i}}_h^* \times\right]^2 \left[\bar{\mathbf{i}}_h \times\right]^2 \left(\frac{\partial \mathbf{r}_h}{\partial \mathbf{r}} - \mathbf{I}_{3\times 3}\right) \left\| \bar{\mathbf{i}}_h + \frac{\bar{\mathbf{v}}_{pv}}{c} \right\|^{-1} \|\mathbf{r}_h - \mathbf{r}\|^{-1} \\
\frac{\partial \mathbf{i}_s^*}{\partial \mathbf{v}} &= -\frac{1}{c}\left[\bar{\mathbf{i}}_s^* \times\right]^2 \left\| \bar{\mathbf{i}}_s + \frac{\bar{\mathbf{v}}_{sv}}{c} \right\|^{-1} \\
\frac{\partial \mathbf{i}_h^*}{\partial \mathbf{v}} &= -\frac{1}{c}\left[\bar{\mathbf{i}}_h^* \times\right]^2 \left\| \bar{\mathbf{i}}_h + \frac{\bar{\mathbf{v}}_{pv}}{c} \right\|^{-1}
\end{aligned}$$

from which we obtain

$$\begin{aligned}
\frac{\partial y_{se}^\star}{\partial \mathbf{r}} &= -\frac{1}{\sin \bar{y}_{se}^\star} \mathbf{i}_s^{*\mathrm{T}} \frac{\partial \mathbf{i}_h^*}{\partial \mathbf{r}} \\
\frac{\partial y_{se}^\star}{\partial \mathbf{v}} &= -\frac{1}{\sin \bar{y}_{se}^\star} \left[\mathbf{i}_h^{*\mathrm{T}} \frac{\partial \mathbf{i}_s^*}{\partial \mathbf{v}} + \mathbf{i}_s^{*\mathrm{T}} \frac{\partial \mathbf{i}_h^*}{\partial \mathbf{v}} \right].
\end{aligned}$$

1. Substellar Point Determination

The star direction $\mathbf{i}_s$ and the position of the vehicle $\mathbf{r}_{pv}$ determine a plane that we can identify with its normal $\mathbf{i}_2$

$$\mathbf{i}_2 = \mathrm{Unit}(\mathbf{i}_s \times \mathbf{r}_{pv}).$$

The intersection of this plane with the horizon is approximately an ellipse, whose semi-major and semi-minor axis are given by

$$\mathbf{i}_0 = \mathrm{Unit}(\mathbf{i}_z \times \mathbf{i}_2) \qquad \mathbf{i}_1 = \mathbf{i}_2 \times \mathbf{i}_0,$$

where $\mathbf{i}_z$ points to the north pole. The inclination of the horizon plane with respect to the equatorial plane is given by

$$\iota = \arcsin \mathbf{i}_1 \cdot \mathbf{i}_z.$$

The rotation matrix from the inertial coordinate system to the horizon coordinate system is given by $\mathbf{T}_i^h$

$$\mathbf{T}_i^h = \begin{bmatrix} \mathbf{i}_0 & \mathbf{i}_1 & \mathbf{i}_2 \end{bmatrix}^{\mathrm{T}}.$$

Let indicate the vectors with components expressed in the horizon coordinate system with an superscript h

$$\mathbf{r}_{pv}^h = \begin{bmatrix} x^h \\ y^h \\ 0 \end{bmatrix} = \mathbf{T}_i^h \, \mathbf{r}_{pv} \qquad \mathbf{i}_s^h = \mathbf{T}_i^h \, \mathbf{i}_s.$$

Define vectors $\mathbf{t}_0$ and $\mathbf{t}_1$ to be tangent to the ellipse and passing through the point $(x_h,\, y_h)$, the vectors are given by

$$\mathbf{t}_i = \frac{1}{d} \begin{bmatrix} x_h \pm (a_h/b_h) y_h \sqrt{d-1} \\ y_h \mp (b_h/a_h) x_h \sqrt{d-1} \\ 0 \end{bmatrix} \qquad i = 1, 2$$

where

$$d = \frac{(x^h)^2}{a_h^2} + \frac{(y^h)^2}{b_h^2}.$$

Scalars a_h and b_h are the semi-major and semi-minor axis of the horizon ellipse. The semi-minor axis is always equal to the planet's semi-minor axis, while a_h is a function of the planet's equatorial and polar radii and the inclination ι

$$\begin{aligned}
a_h &= \left(\frac{\cos^2 \iota}{a_p^2} + \frac{\sin^2 \iota}{b_p^2} \right)^{-\frac{1}{2}} & \iota &= \arcsin \mathbf{i}_1 \cdot \mathbf{i}_z \\
\frac{\partial a_h}{\partial \mathbf{r}} &= a_h^3 \cos \iota \, \sin \iota \left(\frac{1}{a_p^2} - \frac{1}{b_p^2} \right) \frac{\partial \iota}{\partial \mathbf{r}} & \frac{\partial \iota}{\partial \mathbf{r}} &= \frac{1}{\cos \iota} \mathbf{i}_z^{\mathrm{T}} \frac{\partial \mathbf{i}_1}{\partial \mathbf{r}},
\end{aligned}$$

where a_p and b_p are the planet's semi-major and semi-minor axis, respectively, and the partials of $\mathbf{i}_1$ are given in Eq. (11). Vectors $\mathbf{t}_0$ and $\mathbf{t}_1$ correspond to the two horizon points, near horizon or far horizon. The horizon vector to be used by the navigation system is therefore

$$\mathbf{r}_h = \mathbf{T}_h^i \mathbf{t}_i \tag{10}$$

using either $\mathbf{t}_0$ or $\mathbf{t}_1$ whichever corresponds to the near horizon.

2. Substellar Point Partials

The partial of Eq. (10) is given by

$$\frac{\partial \mathbf{r}_h}{\partial \mathbf{r}} = t_i(1)\frac{\partial \mathbf{i}_0}{\partial \mathbf{r}} + t_i(2)\frac{\partial \mathbf{i}_1}{\partial \mathbf{r}} + \mathbf{T}_h^i \frac{\partial \mathbf{t}_i}{\partial \mathbf{r}}.$$

where the partials of the unit vectors are given by

$$\begin{aligned}
\frac{\partial \mathbf{i}_2}{\partial \mathbf{r}} &= -[\mathbf{i}_2\times]^2[\mathbf{i}_s\times]\|\mathbf{i}_s \times \mathbf{r}_{pv}\|^{-1} \\
\frac{\partial \mathbf{i}_0}{\partial \mathbf{r}} &= -[\mathbf{i}_0\times]^2[\mathbf{i}_z\times]\frac{\partial \mathbf{i}_z}{\partial \mathbf{r}}\|\mathbf{i}_z \times \mathbf{i}_2\|^{-1} \\
\frac{\partial \mathbf{i}_1}{\partial \mathbf{r}} &= [\mathbf{i}_2\times]\frac{\partial \mathbf{i}_0}{\partial \mathbf{r}} - [\mathbf{i}_0\times]\frac{\partial \mathbf{i}_2}{\partial \mathbf{r}}.
\end{aligned} \tag{11}$$

We also have that

$$\frac{\partial d}{\partial x^h} = 2\frac{x^h}{a_h^2} \qquad \frac{\partial d}{\partial y^h} = 2\frac{y^h}{b_h^2} \qquad \frac{\partial d}{\partial a_h} = -2\frac{(x_{pv}^h)^2}{a_h^3},$$

and

$$\begin{aligned}
\frac{\partial t_i(1)}{\partial x^h} &= \frac{1}{d} & \frac{\partial t_i(1)}{\partial y^h} &= \pm\frac{\sqrt{d-1}}{d}(a_h/b_h) & \frac{\partial t_i(1)}{\partial a_h} &= \pm\frac{\sqrt{d-1}}{d}(y^h/b_h) \\
\frac{\partial t_i(2)}{\partial y^h} &= \frac{1}{d} & \frac{\partial t_i(2)}{\partial x^h} &= \mp\frac{\sqrt{d-1}}{d}(b_h/a_h) & \frac{\partial t_i(2)}{\partial a_h} &= \pm\frac{\sqrt{d-1}}{d}x^h(b_h/a_h^2)
\end{aligned}$$

$$\frac{\partial \mathbf{t}_i}{\partial d} = -\frac{1}{d}\mathbf{t}_i \pm \begin{bmatrix} (a_h/b_h)y_h \\ -(b_h/a_h)x_h \\ 0 \end{bmatrix} \frac{1}{2d\sqrt{d-1}}.$$

We finally obtain that

$$\frac{\partial \mathbf{t}_i}{\partial \mathbf{r}} = \left(\frac{\partial \mathbf{t}_i}{\partial x^h} + \frac{\partial \mathbf{t}_i}{\partial d}\frac{\partial d}{\partial x^h}\right)\frac{\partial x^h}{\partial \mathbf{r}} + \left(\frac{\partial \mathbf{t}_i}{\partial y^h} + \frac{\partial \mathbf{t}_i}{\partial d}\frac{\partial d}{\partial y^h}\right)\frac{\partial y^h}{\partial \mathbf{r}} + \left(\frac{\partial \mathbf{t}_i}{\partial a_h} + \frac{\partial \mathbf{t}_i}{\partial d}\frac{\partial d}{\partial a_h}\right)\frac{\partial a_h}{\partial \mathbf{r}},$$

where

$$\begin{aligned}
\frac{\partial x^h}{\partial \mathbf{r}} &= \mathbf{r}_{pv}^{\mathrm{T}}\frac{\partial \mathbf{i}_0}{\partial \mathbf{r}} + \mathbf{i}_0^{\mathrm{T}} \\
\frac{\partial y^h}{\partial \mathbf{r}} &= \mathbf{r}_{pv}^{\mathrm{T}}\frac{\partial \mathbf{i}_1}{\partial \mathbf{r}} + \mathbf{i}_1^{\mathrm{T}}.
\end{aligned}$$

B. Apparent Angular Radius Measurement

Let R_p be the actual radius of the planet, the sensed radius of the planet is corrupted by two errors: b_h (the horizon determination bias) and η_R (error due to the horizon determination noise).

$$R_{p,meas} = R_p + b_h + \eta_R.$$

In order to characterize the measurement noise statistics, a simplified algorithm to determine the radius is used. The sensor software would employ many points on the planet disk to determine the radius. For this analysis only three points will be used. The assumption is that by using more points the error in reconstructing the planet radius will decrease, but the shape of the curves will stay the same. Hence our approach is more conservative, in line with this analysis.

Let $\mathbf{p}_i = [x_i \ y_i]^{\mathrm{T}}$ $i = 1:3$ be three points non aligned. To find the coordinates of the center of the circle passing through the three points, we use two cords passing through the points. The center is the interception between the two lines perpendicular to the cords and passing through the cords' mid point. Mathematically the center is

$$x_c = \frac{m_a m_b (y_1 - y_3) + m_b (x_1 + x_2) - m_a (x_2 + x_3)}{2(m_b - m_a)}$$
$$y_c = \frac{(x_1 - x_3) + m_a (y_1 + y_2) - m_b (y_2 + y_3)}{2(m_a - m_b)},$$

where

$$m_a = \frac{y_2 - y_1}{x_2 - x_1} \qquad\qquad m_b = \frac{y_3 - y_2}{x_3 - x_2}. \tag{12}$$

The order of the points is chosen such that the denominators in Eq. (12) do not vanish. Once the center in known, the radius follows immediately as the distance between the center and any of the three points. Consider the case when the three points are not perfect measurements, but contain a radial error. Assume that the true value of the radius changes, but the radial errors remain constant. In this scenario the three points are moved radially by the same amount and the location of the calculated center will remain the same. Therefore we conclude that the estimation error of the radius is independent from the true radius, this intuition is confirmed from the numerical data. Let φ be the angle describing the arc of the planet disk inside the field of view. The three points are equally spaced along the arc. Under these hypothesis the estimation error is only a function of φ and the accuracy of the sensor to locate points on the planet's limb η_h

$$\eta_R = f_1(\varphi, \eta_h).$$

Let σ_R be the standard deviation of η_R, and σ_h the standard deviation of η_h. In order to model σ_R Monte Carlo runs are used. The location of each point is corrupted with a zero-mean, gaussian radial error with standard deviation ranging from 1Km to 15Km. There is no error in the position of the point along the arc. It is assumed that the length of the planet's arc inside the field of view ranges from 45 degrees to 240 degrees. There is no need to simulate arcs bigger than 240 degrees because in those cases the three points will still be placed 120 degrees apart.

Ten thousand Monte Carlo runs where performed for each case. Every run has a different circle center, location and error of the three points. Figure 3 shows the sample standard deviation for ranges between 90 and 240 degrees, the sample mean is very close to zero.

From figure 3, it can be seen that the curves are proportional to σ_h. Therefore we can represent σ_R as

$$\frac{\sigma_R}{\sigma_h} = f_2(\varphi).$$

Function f_2 is expanded in series

$$f_2(\varphi) \simeq \sum_{i=0}^{n} c_i \varphi^{-i},$$

the coefficients c_i are obtained using least squares. For $n = 5$ the coefficient were found to be

$$\mathbf{c} = \begin{bmatrix} 1.8911 & -12.5306 & 33.3895 & -19.3107 & 5.7692 \end{bmatrix}^{\mathrm{T}}.$$

Let ρ be the apparent angular radius of the planet, and R_p the actual radius. Then ρ is given by

$$\rho = \arcsin\left(\frac{R_p}{r_{vp}}\right),$$

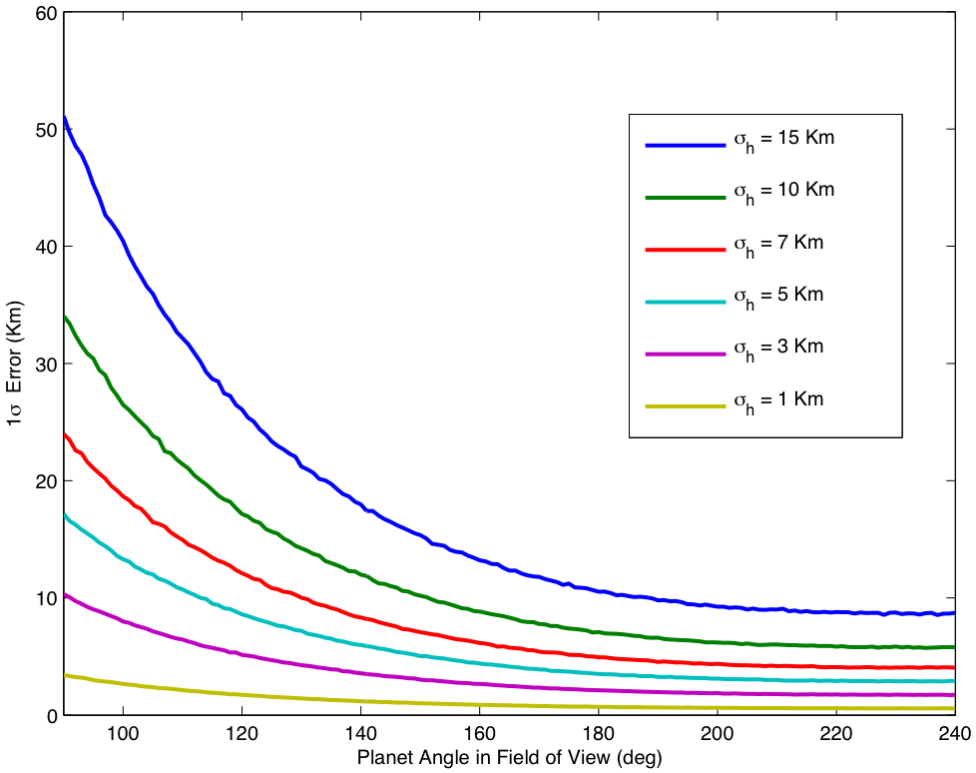

Figure 3. Monte Carlo analysis of apparent angular radius measurement.

where $r_{vp} = \|\mathbf{r} - \mathbf{r}_p\|$ is the distance between the vehicle and the center of the planet. The angular radius measurement y_ρ is given by

$$y_\rho = \arcsin\left(\frac{R_p + b_h + \eta_R}{r_{vp}}\right),$$

the jacobian is given by

$$\mathbf{H}_\rho(1:3) \triangleq \left.\frac{\partial y_\rho}{\partial \mathbf{r}}\right|_{\bar{\mathbf{x}}} = \frac{-R_p - \bar{b}_h}{\sqrt{1 - \left(\frac{R_p + \bar{b}_h}{\bar{r}_{vp}}\right)^2}} \frac{\bar{\mathbf{r}}^{\mathrm{T}} - \mathbf{r}_p^{\mathrm{T}}}{\bar{r}_{vp}^3} \tag{13}$$

$$\mathbf{H}_\rho(4) \triangleq \left.\frac{\partial y_\rho}{\partial b_h}\right|_{\bar{\mathbf{x}}} = \frac{1/\bar{r}_{vp}}{\sqrt{1 - \left(\frac{R_p + \bar{b}_h}{\bar{r}_{vp}}\right)^2}}, \tag{14}$$

where vector $\mathbf{r}$ is the position of the spacecraft, and $\mathbf{r}_p$ is the position of the planet. The indexes 1 to 4 were used because only the active states were included $\mathbf{x}^{\mathrm{T}} = \begin{bmatrix}\mathbf{r}^{\mathrm{T}} & b_h\end{bmatrix}$.

Hence, a Kalman filter that process the measurement y_ρ will employ Eqs. (13)-(14) to obtain the measurement mapping matrix, and will use

$$R_\rho = \frac{\sigma_h^2/\bar{r}_{vp}^2}{1 - \left(\frac{R_p + \bar{b}_h}{\bar{r}_{vp}}\right)^2} \left(\sum_{i=0}^{n} c_i \varphi^{-i}\right)^2$$

as the measurement covariance.

C. Implementation

After the rotational maneuver, Orion is nominally oriented such that the edge of the Earth or moon is at the center of the star camera field of view (FOV). Two cases may arise, the angular radius of the planet as

seen from Orion's position is bigger than the FOV or it is smaller. The first case is depicted in Figure 4, where an isosceles triangle is drawn with $b = c = \rho$ and $a = FOV$, where ρ is the apparent angular radius of the planet. Using the cosine theorem

$$\cos\beta = \frac{a^2 + c^2 - b^2}{2ac} = \frac{FOV}{2\rho}. \tag{15}$$

The smaller triangle is also isosceles, therefore we immediately deduce that the semi-angle of the planet's

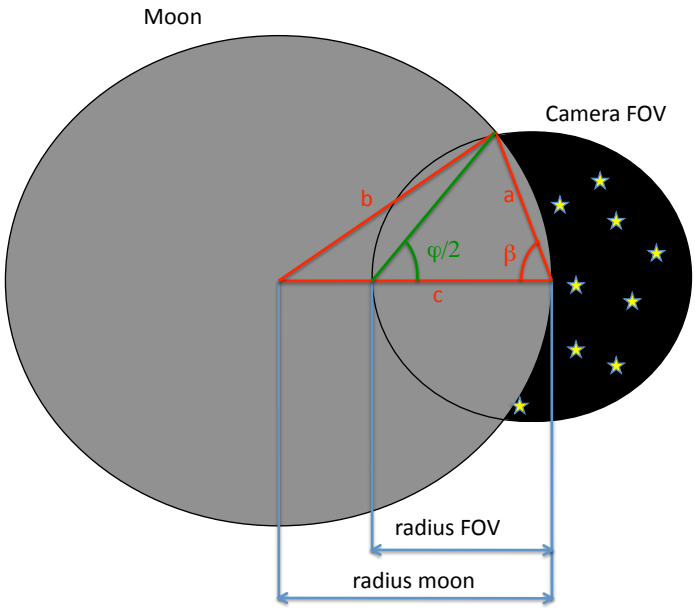

Figure 4. Planet bigger than FOV

arc inside the FOV $\varphi/2$ is (in radiants)

$$\varphi/2 = \frac{\pi - \beta}{2}.$$

Figure 5 shows the case in which the angular radius of the planet is smaller that the star camera FOV. The angle β is still found using Eq. (15), and $\varphi/2$ is simply given by

$$\varphi/2 = \pi - 2\beta.$$

If φ is greater than 240 degrees it is set it is set to be equal to 240 degrees. Notice that by using this model we are adding conservatism because the FOV will probably be square and not circular, which will increase its dimentions.

V. LinCov Parameters

This section contains all the parameters used in the LinCov run.

A. Nominal Trajectory

The nominal trajectory used is that of reference.[5] The initial and final conditions are given in table 1.

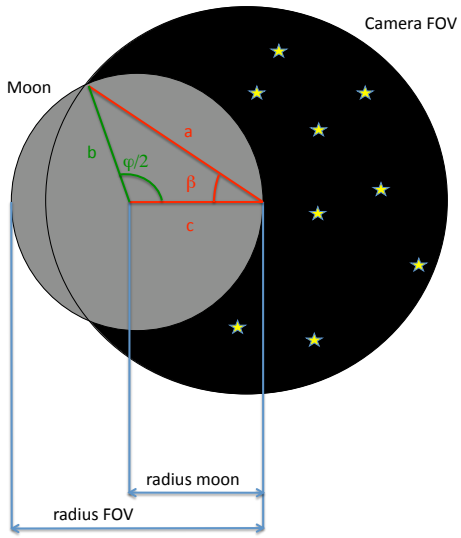

Figure 5. Planet smaller than FOV

	Initial Lunar Orbit	Conditions at EI
Julian Date	2458333.219569300	2458337.833333333
ECI X pos (nm)	202172.039471687	-3183.41601631396
ECI Y pos (nm)	59075.1443050105	-936.33901957676
ECI Z pos (nm)	5581.07932702362	-1143.4480599012
ECI X vel (ft/s)	-1331.89465681683	1911.0234778515
ECI Y vel (ft/s)	5557.26415113373	-24481.9647170493
ECI Z vel (ft/s)	5792.67629243573	26413.8963068702

Table 1. Nominal initial and final conditions

B. Initial Errors and Dispersions

The initial environment dispersion and estimation error are chosen to have the same numerical values as shown in table 2 where the error components are expressed in the local vertical local horizontal frame.

STATE	VARIANCE
LVLH x position	1603 m
LVLH y position	333 m
LVLH z position	1000 m
LVLH x velocity	0.9466 m/s
LVLH y velocity	0.5 m/s
LVLH z velocity	1.61 m/s

Table 2. Initial state variances

C. Process Noise

The Orion vehicle is required to to have quiescent times in which all possible trajectory perturbing activities are reduced to a minimum. For example urine damps, maneuvers, etc are not permitted during these times. Quiescent periods mostly coincide with the astronauts sleeping schedule. In this simulation we use two values of process noise one for active periods and one for quiescent, as shown in table 3. Table 4 shows the quiescent time schedule.

ERROR TYPE	VALUE
Active ($\mu g\sqrt{s}$)	20
Quiescent ($\mu g\sqrt{s}$)	2

Table 3. Process noise values

BEGIN QUIESCENT TIME	END QUIESCENT TIME
TEI-1 + 3 hrs	TEI-1 + 11 hrs
TEI-3 + 3.5 hrs	TEI-3 + 11.5 hrs
TEI-3 + 25 hrs	TEI-3 + 33 hrs
TEI-3 + 47 hrs	TEI-3 + 55 hrs
EI - 14 hrs	EI - 7 hrs

Table 4. Quiescent time schedule

D. Maneuvers Errors

Table 5 shows the six planned maneuvers during Earth return. Moon departure is performed with a sequence of three trans-Earth injection maneuvers (TEI 1 to 3). Three trajectory correction maneuvers (TCM 1 to 3) are also performed. Times are expressed as hours from the beginning of the simulation which occurs 1.11 days before TE3. Table 6 shows the maneuver errors used in the simulation (all values are 1σ per axis)

MANEUVER	TIME (hr)	$\Delta\mathbf{v}$ (m/s)
TEI-1	2.68	$\begin{bmatrix}439.0000456858 & -255.14643452537 & -261.37312482242\end{bmatrix}$
TEI-2	17.84	$\begin{bmatrix}29.380624008588 & 100.42253852018 & -96.0532565591\end{bmatrix}$
TEI-3	26.73	$\begin{bmatrix}264.61950434635 & -206.66625626422 & 23.2732316094037\end{bmatrix}$
TCM-1	44.73	nominally zero
TCM-2	94.73	nominally zero
TCM-3	105.73	nominally zero

Table 5. Trans-Earth maneuver sequence

ERROR TYPE	VALUE
Misalignment (deg)	0.01
Bias (m/s)	0.001
Scale factor (ppm)	10
Noise (m/s)	0.001

Table 6. Trans-Earth maneuver errors

E. Measurement Accuracy

The values used for the horizon and substellar point errors are those from Apollo and are shown in table 7.

ERROR TYPE	MOON	EARTH
star camera		
η_{sc} (arcsec) 3σ	15	15
b_{sc} (arcsec) 3σ	10	10
stellar subpoint		
η_{ss} (arcsec) 1σ	5	10
b_{ss}(arcsec) 1σ	2	5
horizon		
η_h (km) 1σ	5	10
b_h (km) 1σ	3	3

Table 7. Star elevation measurement errors

VI. Event Triggers

Using linear covariance techniques events are usually time driven. Some events, like EI, are naturally defined by the state and not by time. The technique to introduce these events into LinCov are those presented in reference 6 with some modifications due to the fact that the definer is the true state and not the navigated state.

Let the event be defined by some function of the state

$$\Psi(\mathbf{x}) = 0 \tag{16}$$

The true state at the true event time (t_e) differs from the nominal state at the nominal event time ($\bar{t}_e$) because of differences in both state and time

$$\mathbf{x}(t_e) \simeq \mathbf{x}(\bar{t}_e) + \dot{\mathbf{x}}(\bar{t}_e)[t_e - \bar{t}_e] \tag{17}$$

$$\hat{\mathbf{x}}(t_e) \simeq \hat{\mathbf{x}}(\bar{t}_e) + \dot{\hat{\mathbf{x}}}(\bar{t}_e)[t_e - \bar{t}_e], \tag{18}$$

where

$$\dot{\mathbf{x}}(\bar{t}_e) = \dot{\bar{\mathbf{x}}}(\bar{t}_e) + \delta\dot{\mathbf{x}}(\bar{t}_e) \tag{19}$$

$$\dot{\hat{\mathbf{x}}}(\bar{t}_e) = \dot{\bar{\mathbf{x}}}(\bar{t}_e) + \delta\dot{\hat{\mathbf{x}}}(\bar{t}_e). \tag{20}$$

Expanding Eq. (16) we obtain

$$0 = \Psi(\bar{\mathbf{x}}(\bar{t}_e)) + \mathbf{\Psi}_x[\delta\mathbf{x}(\bar{t}_e) + \dot{\bar{\mathbf{x}}}(\bar{t}_e)\delta t_e]$$

where

$$\mathbf{\Psi}_x \triangleq \left.\frac{\partial\Psi}{\partial\mathbf{x}}\right|_{\bar{\mathbf{x}}} \qquad\qquad \delta t_e \triangleq t_e - \bar{t}_e.$$

Noticing that $\Psi(\bar{\mathbf{x}}(\bar{t}_e)) = 0$ we can solve for δt_e

$$\delta t_e = -\frac{\mathbf{\Psi}_x\,\delta\mathbf{x}(\bar{t}_e)}{\mathbf{\Psi}_x\dot{\bar{\mathbf{x}}}(\bar{t}_e)},$$

substituting into Eqs. (17-18), using Eqs. (19-20) and neglecting second order terms we obtain

$$\mathbf{x}(t_e) \simeq \mathbf{x}(\bar{t}_e) - \dot{\bar{\mathbf{x}}}(\bar{t}_e)\frac{\mathbf{\Psi}_x\,\delta\mathbf{x}(\bar{t}_e)}{\mathbf{\Psi}_x\dot{\bar{\mathbf{x}}}(\bar{t}_e)}$$

$$\hat{\mathbf{x}}(t_e) \simeq \hat{\mathbf{x}}(\bar{t}_e) - \dot{\bar{\mathbf{x}}}(\bar{t}_e)\frac{\mathbf{\Psi}_x\,\delta\mathbf{x}(\bar{t}_e)}{\mathbf{\Psi}_x\dot{\bar{\mathbf{x}}}(\bar{t}_e)}.$$

Let define

$$\mathbf{U} \triangleq \frac{\dot{\bar{\mathbf{x}}}(\bar{t}_e)\mathbf{\Psi}_x}{\mathbf{\Psi}_x \dot{\bar{\mathbf{x}}}(\bar{t}_e)}.$$

We are interested in knowing the difference between the true/nav state at the time of the event and the nominal state at the nominal time of the event

$$\begin{aligned}
\delta\mathbf{x}(t_e) &= \mathbf{x}(t_e) - \bar{\mathbf{x}}(\bar{t}_e) = (\mathbf{I} - \mathbf{U})\,\delta\mathbf{x}(\bar{t}_e) \\
\delta\hat{\mathbf{x}}(t_e) &= \hat{\mathbf{x}}(t_e) - \bar{\mathbf{x}}(\bar{t}_e) = \delta\hat{\mathbf{x}}(\bar{t}_e) - \mathbf{U}\delta\mathbf{x}(\bar{t}_e) \\
\mathbf{e}(t_e) &= \mathbf{e}(\bar{t}_e),
\end{aligned}$$

therefore to first order the estimation error remains unchanged. Notice that t_e is a random variable and not a deterministic time and that the dispersions are still unbiased therefore it makes sense to talk about covariances.[6] The augmented covariance at the event (no precise time can be attributed to this covariance) is given by

$$\mathbf{\Pi}_e = \begin{bmatrix} \mathbf{I} - \mathbf{U} & \mathbf{O} \\ -\mathbf{U} & \mathbf{I} \end{bmatrix} \mathbf{\Pi}(\bar{t}_e) \begin{bmatrix} \mathbf{I} - \mathbf{U} & \mathbf{O} \\ -\mathbf{U} & \mathbf{I} \end{bmatrix}^{\mathrm{T}}$$

A. Entry Interface

Entry interface is defined as a constant altitude $h_{EI} = 400000$ feet, therefore function Ψ is equal to

$$\mathbf{r}^{\mathrm{T}}\mathbf{r} - (h_{EI} + R_{EARTH})^2 = 0.$$

Let $\bar{\mathbf{x}}_{EI}$ be the nominal state at entry interface, then matrix $\mathbf{U}$ at EI is

$$\mathbf{U}_{EI} = \frac{1}{\bar{\mathbf{r}}_{EI}^{\mathrm{T}}\bar{\mathbf{v}}_{EI}} \begin{bmatrix} \dot{\bar{\mathbf{x}}}_{EI}\bar{\mathbf{r}}_{EI}^{\mathrm{T}} & \mathbf{O} \end{bmatrix}.$$

Notice that there is no radial uncertainty in the environment dispersion since the dispersion is perpendicular to $\bar{\mathbf{r}}_{EI}$

$$\bar{\mathbf{r}}_{EI}^{\mathrm{T}}\delta\mathbf{r}_{EI} = \bar{\mathbf{r}}_{EI}^{\mathrm{T}} \left(\mathbf{I} - \frac{\bar{\mathbf{v}}_{EI}\bar{\mathbf{r}}_{EI}^{\mathrm{T}}}{\bar{\mathbf{r}}_{EI}^{\mathrm{T}}\bar{\mathbf{v}}_{EI}} \right) \delta\mathbf{r}(\bar{t}_{EI}) = \left(\bar{\mathbf{r}}_{EI}^{\mathrm{T}} - \bar{\mathbf{r}}_{EI}^{\mathrm{T}} \right) \delta\mathbf{r}(\bar{t}_{EI}) = 0$$

this is to be expected since at the event the altitude is fixed and equal to h_{EI}.

VII. Results

In this section the result of numerical simulations are shown. Targeting occurs approximately 45 minutes before the maneuver. In this simulation the vehicle is rotated to acquire measurements 2 hours before the maneuver and takes 60 measurements 1 minute apart. Measurement acquisition also occurs between the second and third midcourse correction, more precisely at 60 and 80 hours from the beginning of the simulation.

A. Flight Path Angle

The single most important parameter to assure crew safety during entry is the flight path angle γ

$$\gamma = \arcsin \frac{\mathbf{r}^{\mathrm{T}}\mathbf{v}}{\|\mathbf{r}\|\,\|\mathbf{v}\|}.$$

The flight path angle onboard error covariance is approximately given by,

$$P_{\gamma\gamma} = \begin{bmatrix} \frac{\partial\gamma}{\partial\mathbf{r}}(\bar{\mathbf{r}},\bar{\mathbf{v}}) & \frac{\partial\gamma}{\partial\mathbf{v}}(\bar{\mathbf{r}},\bar{\mathbf{v}}) \end{bmatrix} \begin{bmatrix} \mathbf{P}_{rr} & \mathbf{P}_{rv} \\ \mathbf{P}_{vr} & \mathbf{P}_{vv} \end{bmatrix} \begin{bmatrix} \frac{\partial\gamma}{\partial\mathbf{r}}^{\mathrm{T}}(\bar{\mathbf{r}},\bar{\mathbf{v}}) \\ \frac{\partial\gamma}{\partial\mathbf{v}}^{\mathrm{T}}(\bar{\mathbf{r}},\bar{\mathbf{v}}) \end{bmatrix}, \tag{21}$$

where

$$\frac{\partial\gamma}{\partial\mathbf{r}} = \frac{1}{\cos\gamma} \frac{\mathbf{v}^{\mathrm{T}}}{\|\mathbf{r}\|\,\|\mathbf{v}\|} \left(\mathbf{I} - \frac{\mathbf{r}\mathbf{r}^{\mathrm{T}}}{\|\mathbf{r}\|^2} \right) \qquad \frac{\partial\gamma}{\partial\mathbf{v}} = \frac{1}{\cos\gamma} \frac{\mathbf{r}^{\mathrm{T}}}{\|\mathbf{r}\|\,\|\mathbf{v}\|} \left(\mathbf{I} - \frac{\mathbf{v}\mathbf{v}^{\mathrm{T}}}{\|\mathbf{v}\|^2} \right).$$

Notice that we are not interested in the flight path angle uncertainty at each given time, but we are interested in that uncertainty mapped to entry interface. For example, if at the time of the last maneuver our flight path angle onboard uncertainty mapped to EI is 0.5 degrees 3σ, we can not achieve a better environment dispersion than that at EI, the uncertainty will actually be bigger due to acceleration perturbations, burn errors, targeting errors, etcetera. Therefore there are two values that we are interested in, the onboard uncertainty at the time of the last maneuver, and the environment dispersion at the time of entry interface. The first has to be able to guide us safely to EI, the second tells us if we met the safety conditions.

The plots presented in this section show the flight path angle error mapped at EI, to do that we propagate the covariance to the final time with the state transition matrix and we evaluate the partials at the nominal value at EI. Denote $P_{\gamma\gamma}(t_{EI}, t)$ the onboard variance of the flight path angle error mapped to entry interface, then we obtain from Eq. (21)

$$P_{\gamma\gamma}(t_{EI},t) = \begin{bmatrix} \frac{\partial\gamma}{\partial\mathbf{r}} & \frac{\partial\gamma}{\partial\mathbf{v}} \end{bmatrix}_{\bar{\mathbf{r}}_{EI},\bar{\mathbf{v}}_{EI}} \mathbf{\Phi}(t_{EI},t) \begin{bmatrix} \mathbf{P}_{rr}(t) & \mathbf{P}_{rv}(t) \\ \mathbf{P}_{vr}(t) & \mathbf{P}_{vv}(t) \end{bmatrix} \mathbf{\Phi}(t_{EI},t)^{\mathrm{T}} \begin{bmatrix} \frac{\partial\gamma}{\partial\mathbf{r}}^{\mathrm{T}} \\ \frac{\partial\gamma}{\partial\mathbf{v}}^{\mathrm{T}} \end{bmatrix}_{\bar{\mathbf{r}}_{EI},\bar{\mathbf{v}}_{EI}},$$

where $\mathbf{\Phi}$ is the state 6×6 transition matrix of position and velocity, and the partials are evaluated at the nominal state at EI. Similarly we can obtain the dispersions augmented variances as

$$\bar{P}_{\gamma\gamma}(t_{EI},t) = \begin{bmatrix} \frac{\partial\gamma}{\partial\mathbf{r}} & \frac{\partial\gamma}{\partial\mathbf{v}} \end{bmatrix}_{\bar{\mathbf{r}}_{EI},\bar{\mathbf{v}}_{EI}} \mathbf{U}_{EI}\mathbf{\Phi}(t_{EI},t) \begin{bmatrix} \bar{\mathbf{P}}_{rr}(t) & \bar{\mathbf{P}}_{rv}(t) \\ \bar{\mathbf{P}}_{vr}(t) & \bar{\mathbf{P}}_{vv}(t) \end{bmatrix} \mathbf{\Phi}(t_{EI},t)^{\mathrm{T}}\mathbf{U}_{EI}^{\mathrm{T}} \begin{bmatrix} \frac{\partial\gamma}{\partial\mathbf{r}}^{\mathrm{T}} \\ \frac{\partial\gamma}{\partial\mathbf{v}}^{\mathrm{T}} \end{bmatrix}_{\bar{\mathbf{r}}_{EI},\bar{\mathbf{v}}_{EI}}$$

$$\hat{P}_{\gamma\gamma}(t_{EI},t) = \begin{bmatrix} \frac{\partial\gamma}{\partial\mathbf{r}} & \frac{\partial\gamma}{\partial\mathbf{v}} \end{bmatrix}_{\bar{\mathbf{r}}_{EI},\bar{\mathbf{v}}_{EI}} \mathbf{U}_{EI}\mathbf{\Phi}(t_{EI},t) \begin{bmatrix} \hat{\mathbf{P}}_{rr}(t) & \hat{\mathbf{P}}_{rv}(t) \\ \hat{\mathbf{P}}_{vr}(t) & \hat{\mathbf{P}}_{vv}(t) \end{bmatrix} \mathbf{\Phi}(t_{EI},t)^{\mathrm{T}}\mathbf{U}_{EI}^{\mathrm{T}} \begin{bmatrix} \frac{\partial\gamma}{\partial\mathbf{r}}^{\mathrm{T}} \\ \frac{\partial\gamma}{\partial\mathbf{v}}^{\mathrm{T}} \end{bmatrix}_{\bar{\mathbf{r}}_{EI},\bar{\mathbf{v}}_{EI}}$$

Figures 6–7 show the numerical results. It can be seen that the navigation system meet the requirements.

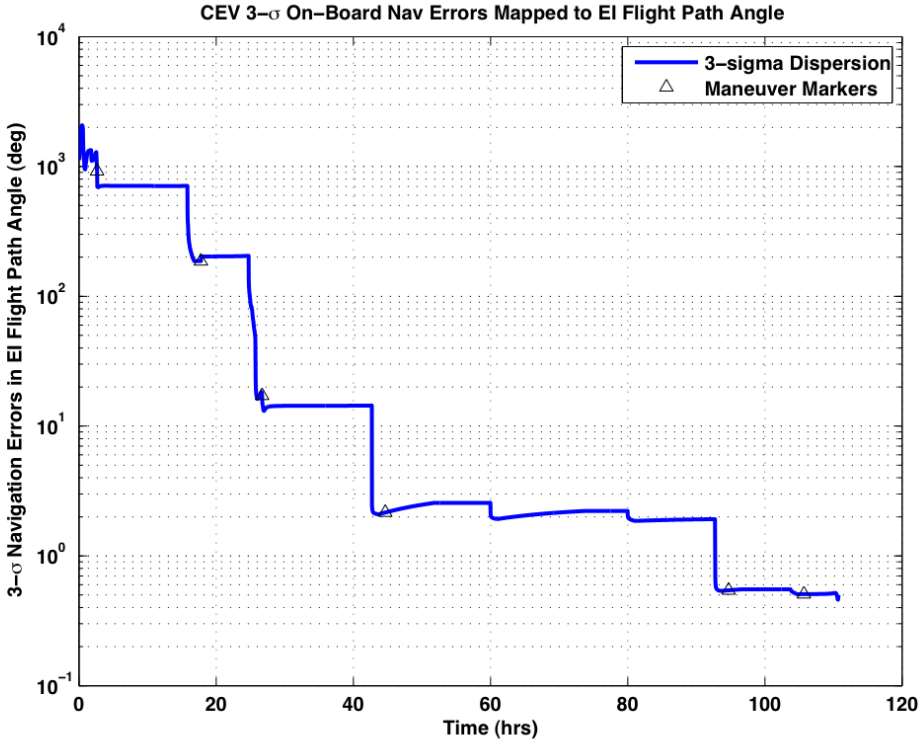

Figure 6. Onboard Flight path angle error mapped to entry interface

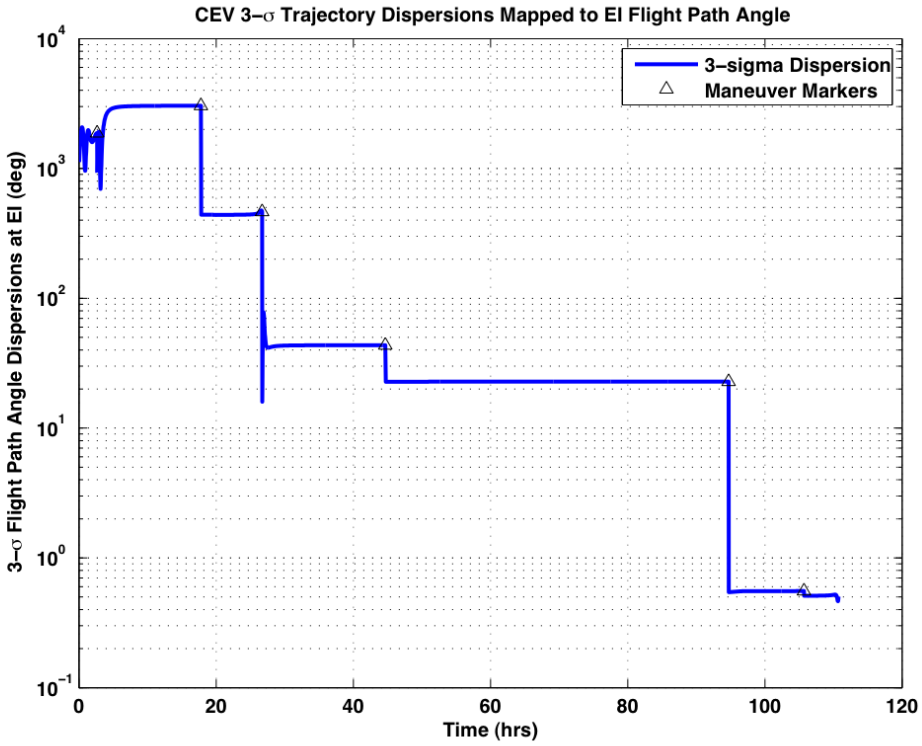

Figure 7. True Flight path angle error mapped to entry interface

VIII. Conclusion

An optical only navigation solution was presented for lunar return. It was shown that this architecture is able to meet flight path angle requirements for a safe direct entry.

References

[1]Gelb, A., editor. "Applied Optimal Estimation" The MIT press, Massachusetts Institute of Technology, Cambridge, MA, 1996.

[2]Geller, D., "Linear Covariance Techniques for Orbital Rendezvous Analysis and Autonomous Onboard Mission Planing," AIAA Guidance, Navigation, and Control Conference, San Francisco, CA, August 2005

[3]D'Souza, C., "An Efficient and Accurate Fized-Step Trajectory Integration Algorithm for Orion," FltDyn-CEV-07-122 NASA, Houston, TX, October 25 2007.

[4]Battin, R. H., "An Introduction to the Mathematics and Methods of Astrodynamics", AIAA Education Series, American Institude of Aeronautics and Astronautics, New York, NY, 1987.

[5]Tuckness, D., "DRM-2 Earth/Moon/Earth Reference Trajectories," ESCG-4380-07-AFD-DOC-0001, January 18, 2006.

[6]Geller, D. and Rose, B. and Woffinden, D., "Event Triggeres in Linear Covariance Analysis With Applications to Orbital Rendezvous Analysis," AAS Guidance and Control Conference, Breckenridge, CO, February 2008